An Overview of the Evolution of Method of Moments Techniques in Modern EM Simulators

Carlos Delgado[1, *], Eliseo Garcia[2], Javier Moreno[1], Iván González[1], and Felipe Catedra[1]

(*Invited Paper*)

Abstract—This paper presents an evolution of the challenges and solutions found in the application of techniques based on the Method of Moments until the present day. The original MoM presented very high computational restrictions that have motivated the development of more efficient approaches. The main features of these newer improvements are presented, as well as other technical details regarding preconditioning and parallelization techniques. Some representative examples are shown in order to assert the suitability of these approaches for the analysis of complex and realistic scenarios.

1. INTRODUCTION

Maxwell's equations [1] have been in use for a long time and are a beautifully concise way to teach electrical engineering students about the behavior of electromagnetic waves and their interaction with arbitrary objects. It should be noted, however, that all the modern software packages for electromagnetic simulation have at their core this set of expressions. An enormous range of applications, therefore, depends on the direct application of these equations or on simplifications that allow a faster computation but are limited to some constraints [2, 3]. Such applications include antenna design, propagation analysis, communication systems, radar, on-board antennas, infrared analysis, radome design, circuits and many more.

The Method of Moments (MoM), widely known and used in computational electromagnetics, is easily derived from Maxwell's equations [4]. From the differential formulation of these expressions, applying simple vector calculus identities and introducing the scalar and vector electric and magnetic potentials (ϕ_e, ϕ_m, $\vec{A}$ and $\vec{F}$), the equations of the potentials are easily obtained. At such point the boundary conditions can be applied in order to obtain the electric and magnetic field integral equations, widely known as EFIE and MFIE, respectively. In the first case the cancellation of the tangential electric field on a surface is enforced, while in the second case the total current density equals the tangential component of the magnetic field on the surface. An analogous procedure can be consider to take into account volumetric dielectrics. The Combined Field Integral Equation (CFIE) [5] is also widely used in modern simulation software and it consists of a linear combination of the previous integral equations using the real α parameter defined between 0 and 1 as follows:

$$\text{CFIE} = \alpha \cdot \text{EFIE} + \frac{j}{k}(1 - \alpha) \cdot \text{MFIE} \tag{1}$$

where it is common to find $0.1 \leq \alpha \leq 0.5$ as reference values. As α increases, the convergence may become slower, but the accuracy increases as well. Regarding the properties of these formulations, the EFIE can be used to analyze both open and closed surfaces with a high degree of accuracy, although

* Corresponding author: Carlos Delgado (carlos.delgado@uah.es).

[1] Computer Science Department, University of Alcalá, Spain. [2] Automatics Department, University of Alcalá, Spain.

at very low frequencies it suffers from an imbalanced contribution of the vector potential compared to the scalar potential that renders the EFIE operator ill-conditioned. The EFIE may present as well slow convergence issues due to the non-ideal eigenvalue spectrum of the coupling matrix, with eigenvalues that tend to cluster around the origin. The MFIE, in turn, presents faster convergence properties, although it is limited to the analysis of closed bodies and usually presents lower accuracy than EFIE. The MFIE does not seem to suffer from low-frequency breakdown but its accuracy can be seriously compromised at low frequencies. The CFIE formulation generally addresses undesired internal resonant modes of the cavities formed by the surface of the objects under analysis that appear when analyzing problems using EFIE or CFIE, and it allows the user to adjust the accuracy and the convergence properties by tuning the α parameter.

In order to apply these expressions to obtain the currents over an arbitrary surface given a certain excitation it is necessary to discretize both the geometry and the field equations. The discretization of the geometry allows to obtain a geometrical mesh over which the current basis functions are defined [6, 7]. The discretization of the field equations is performed by introducing the test functions and allow to linearize the electromagnetic problem, which is defined by a coupling (or impedance) matrix.

The legacy application of the Method of Moments is only suitable, however, to analyze small problems due to the necessity of storing the full coupling matrix and performing the necessary operations to solve the problem for a given excitation. In this context there are a number of approaches derived in more recent years which are headed towards a relaxation of the computational strain posed by the MoM. This is achieved mainly by following two lines: (i) avoiding the storage of the complete coupling matrix and (ii) performing fast matrix-vector products in an iterative solver in order to increase the computational efficiency. A third line of work, not incompatible with the previous ones, consists of the reduction of the size of the problem by using special sets of basis functions. These enhancements of the legacy MoM are discussed with more detail in Section 2.

Section 3 addresses the importance and the use of direct and iterative solvers in modern implementations of EM simulators. Even though direct solvers may be preferred for very small problems, especially with multiple excitations, iterative solvers will be overwhelmingly predominant, and it is very important to introduce preconditioning strategies in order to reduce the solving time required, especially when dealing will ill-conditioned problems. The quality of the mesh is also a key factor in the solution process.

Section 4 deals with details regarding the parallelization of the previously discussed techniques. It is worthwhile that, aside from the novel efficient numerical techniques developed in the last years, computational electromagnetics has taken advantage of the rapid increase in computational power, in terms of CPU speed and memory available among other factors, which allows to simulate scenarios on general purpose computers nowadays that could only be approached using workstations some years ago. Modern workstations and midsized clusters of computers can deal with problems entailing millions of unknowns. It is easy to realize in this context the huge importance of the parallelization strategies necessary to distribute the computation of the different stages of an arbitrary simulation over a number of processing nodes.

We present in Section 5 some examples simulated using modern methods and covering different applications. The presented results have been obtained taking into account all the details presented in this document.

As a conclusion, Section 6 presents some of the future work lines for the simulation software, as well as a summary of the evolution of the application of Maxwell's equations for the solution of modern problems.

2. IMPROVING THE EFFICIENCY OF THE MOMENT METHOD

As indicated in Section 1, the conventional MoM is not well suited to handle the simulation of electrically medium or large problems, since it is necessary to store the full coupling matrix. As an example, a realistic problem containing one million basis functions would need to store 10^{12} elements, and if each one of them is stored as a simple precision 8 bytes complex number, a total of 8 terabytes of memory would be needed for storage (half that amount if a Galerkin scheme is used, since the coupling matrix is symmetric). This enormous memory size and the time required to fill the matrix render the use of

the conventional MoM totally unfeasible.

A very commonly adopted solution consists of storing only the near-field coupling terms of the matrix, understanding as near-field maximum distances between the basis and test functions of around 0.25 wavelengths. Some popular applications of this procedure include the Multilevel Fast Multipole Algorithm (MLFMA) [8–10], in which the far-field interactions are taken into account in the solver by means of the aggregation of the basis functions into multipole expansions referred to the center of a number of regions, translation of this expansions (and new aggregations to upper levels) and disaggregation of the multipoles over the test functions. It is worthwhile to mention here other family of methods that make use of matrix compression in order to bypass the storage of the far-field coupling terms and speed up the matrix-vector products. This is performed by taking advantage of the fact that a submatrix containing the coupling terms between two distant geometrical blocks will be rank-defficient and therefore it will be possible to represent it with a reduced amount of information. This approach is purely algebraic and therefore independent from the Green's functions. Some approaches such as the Dual Modified Gram Schmidt block-QR-factorization [11] or the block IE-QR approach presented in [12] also offer the advantage of not having to assemble the full submatrix before performing the compression. The Adaptive Cross Approximation method [13] also presents the same advantage and has been extensively studied and applied in the last years, including error and convergence analysis [14, 15], multilevel and hierarchical implementations [16, 17] or combinations with other fast approaches such as MLFMA [18] or the Characteristic Basis Function Method [19].

Other techniques that take advantage of the efficient evaluation of fast matrix-vector products are the Complex Multipole Beam Approach (CMBA) [20], that relies on using a series of beams represented as Gabor functions on the scatterer boundary in order to reduce the size of the matrix under consideration, the combination of the Complex Source Beam and the Moment Method [21], that performs fast matrix-vector products by taking advantage of the directional properties of the Complex Source Beams representing the radiation from the basis elements included in each group, the Impedance Matrix localization (IML) technique [22], which, in turn, aims to sparsify the impedance matrix by introducing special basis and test functions that localize the important interactions to only a small number of elements in the matrix, the Adaptive Integral Method (AIM) [23], which exploits the Toeplitz property of the Green's function kernel to reduce storage and accelerate the matrix-vector products by making use of the Fast Fourier Transform, or the Multilevel Matrix Decomposition Algorithm (MLMDA) [24], that subdivides the MoM matrix into a large number of submatrices, operates on them separately and assembles the solutions in order to achieve faster CPU-times.

A different type of approach that has received wide attention in the last 10 years consists of a reduction of the number of unknowns by using macro-basis functions (MBFs). This reduction is typically around one order of magnitude, which implies a faster solution. The macro-basis functions used in this context are sometimes also called Characteristic Basis Functions or Synthetic Functions [25, 26]. The basic idea underlying this method relies on the generation of the macro-basis functions in a pre-processing stage. In order to generate the MBFs the geometry must be partitioned into blocks, which can have sizes of around several wavelengths. Over each one of these blocks the MBFs will be calculated and tailored to the geometrical description of the block. Each MBF is described internally as an aggregation of low-level, conventional MoM basis functions, and several MBFs coexist over the same block in order to accurately describe the shape of the current over it. The k-th MBF of a given block can be thus expressed in terms of low-level basis functions as:

$$J_k = \sum_{n=1}^{N_k} \alpha_{k,n} T_n \tag{2}$$

where N_k denotes the number of low-level functions over block-k, and T_n stands for the n-th low level basis function on that block. This expression allows to write the coupling between two different MBFs in terms of low-level functions as well, which facilitates the adoption of this approach in legacy MoM codes. The impedance term between the n-th MBF (active) and the m-th MBF (passive) can be written as:

$$\langle L(J_n), W_m \rangle = \sum_{k=1}^{N_m} \sum_{l=1}^{N_n} \alpha_{m,k} \alpha_{n,l}^* \langle T_l, R_k \rangle \tag{3}$$

where W_m can be seen as the test function, and R_k indicates the k-th low-level test function over the block where the m-th MBF belongs.

The generation of the MBFs is performed as follows: the block under study is isolated from the rest of the geometry, and a number of sources are placed around this block. The literature shows that it is possible to use different kinds of sources, like plane waves or dipoles, with equally good results. The currents induced by these sources on the block are then calculated and stored. It is possible to use different methods for this purpose, such as the conventional Method of Moments, the MoM combined with the MLFMA or the Physical Optics (PO) approach if the surface of the block satisfies the constraints imposed by this high-frequency technique [26]. Note that for each block a small independent problem is computed using a number of different excitations. After obtaining all the induced currents, these are used to compute a new base of orthonormal vectors using algebraic techniques such as Gram-Schmidt [25] or the Singular Value Decomposition (SVD) [27]. The reduction of the number of unknowns of the problem, and the key step of the methods based on the use of MBFs, is that the number of functions in the new base can be safely truncated and greatly reduced from the original number of low-level functions in the same block. The magnitude of the singular values from the SVD of the matrix containing all the induced currents on the block shows a rapid fall, which indicates that a relatively small amount of the singular vectors contain all the information to accurately model all the induced currents on the block.

Some considerations shall be remarked at this point concerning the use of MBFs: first, the process described above for the generation of the new set of basis functions requires computation time in addition to the rest of the steps involved in the MoM. The total CPU time, however, makes up for this time overhead in many cases, especially when multiple excitations are to be considered, as in the case of monostatic RCS analysis. For small problems, however, the time reduction may be negligible. Secondly, the reader may note that if the partitioning of the geometry in terms of blocks is performed automatically it will be unavoidable to introduce artificial edges by isolating these blocks later in the MBF computation, and these edges may introduce undesired effects when computing the currents on the blocks. In order to avoid this artificial behavior an extension of the blocks is considered (which is not necessary when the PO approach is used to obtain the currents), the currents are computed over the extended blocks and later the extension is discarded in order to keep the regular behavior of the induced currents before calculating the new base. Some works [28] deal explicitly with the problem of being able to represent the fast variation of the real edge currents with a fewer number of MBFs by introducing specific blocks that contain such edges, and general blocks in those parts where the currents show a regular behavior. Finally, the reduction of the number of unknowns of the problem allows the application of direct solvers in some cases for which an iterative solver is the only viable option when applying MoM-based methods based solely on the use of low-level basis functions. It is necessary to keep in mind, however, that not all the problems might be addressed using direct solvers even with this reduced number of unknowns, and other approaches can be considered [29].

3. SOLUTION OF THE MOM EQUATION

The solution process is very important in modern EM simulators, especially when dealing with large or ill-conditioned problems. This step is usually the most time consuming and the result is the current distribution, in terms of the computed weights of the existing basis functions, over the geometry of the problem. Direct solvers are affordable only in those simulations with a small number of unknowns, and are usually limited to a few tens of thousands. The use of MBFs allows extending the use of direct solvers over this limit, since the conventional MoM matrix is replaced by a reduced matrix. The Scalapack library [30] allows the parallel solution using the Message Passing Interface (MPI) [31] of different kinds of linear systems. An advantage of the use of a direct solver is the fast computation of the solution for different excitations after the factorization of the impedance matrix, as is the case of monostatic RCS problems. For many realistic simulations, however, the use of direct solvers is unfeasible and it is necessary to resort to iterative ones. It is important to mention at this point the Conjugate Gradient Method (CGM) [32], that, despite being only applicable to symmetric and positive definite matrices, has been generalized by the Biconjugate Gradient Stabilized (BiCG-Stab) algorithm [33], which is widely used at the present time. The Generalized Minimal Residual Method (GMRES) [34]

is also a very common choice among the modern iterative solvers in electromagnetics, although the restarted version GMRES(k) is often preferred [35], since the conventional GMRES requires a memory usage that depends on the number of iterations, which may demand an excessive amount of memory in some cases. The restarted versions of the algorithm allow limiting the maximum amount of memory needed in the solution process.

In addition to a suitable solver it is often very necessary to include the use of a preconditioner to speed up the convergence of the solution by improving the condition number while retaining the same solution to the given problem. It is often seen as a matrix that multiplies both sides of the MoM equation:

$$[M] \cdot [Z] \cdot [J] = [M] \cdot [V] \tag{4}$$

It is easy to see that the preconditioner will be more effective as it approaches the inverse of the impedance matrix. Many problems are ill-conditioned, and the use of the EFIE formulation, required when processing open geometries, presents the difficulty of a slower convergence. Different types of preconditioners are available in the literature and they are often dependent on the nature of the numerical method used. It is common, however, to separate the reaction terms that correspond to the near field interactions and the far field interactions:

$$[Z] = [Z_n] + [Z_f] \tag{5}$$

As seen before in this document, $[Z_f]$ is not normally stored, and it is a common practice to build the preconditioners using the near-field part, $[Z_n]$. This matrix contains the strongest elements of $[Z]$ and the use of a preconditioner based on $[Z_n]$ alone assumes the following approximation:

$$[Z_n]^{-1} \cdot [Z] \cong [I] \tag{6}$$

The simplest type of preconditioner is the diagonal preconditioner, and it consists of a diagonal matrix M using the self-interactions. Despite the simplicity of this approach there are enhancements that offer improved performance [36]. The Incomplete LU preconditioner, in turn, is another popular approach based on the approximate LU factorization of Z_n and the use of those factors to perform the operation indicated in (3) [37]. A simple implementation of this preconditioner is denoted as ILU (0), in which the same sparsity pattern as $[Z_n]$ is enforced. More advanced approaches make use of different sparsity patterns that can depend on a threshold used to discard or accept new elements. Obviously, with a higher number of elements the resulting factors involve a closer estimation of $[Z_n]^{-1}$, at the expense of higher CPU-time and storage requirements. A third commonly used choice in modern simulators is the Sparse Approximate Inverse (SAI) preconditioner [38–41], whose goal is the generation of a sparse preconditioning matrix that resembles the inverse matrix $[Z_n]^{-1}$, but using a predefined (or dynamically defined in some cases) sparsity pattern. This preconditioning technique was presented in [38] for dense matrices and has recently received wide attention in the EM community. The SAI preconditioner is generally built using the near-field matrix terms, and solving a linear least-squares (LLS) problem for each one of the basis functions of the scenario. Each one of these least-squares problems yields a new row of the preconditioner, and it is formulated by minimizing the Frobenius norm of the product $[M][Z_n]$. An extremely interesting feature of this procedure is that the whole problem can be decomposed into N independent LLS problems for each one of the N rows of the impedance matrix:

$$\min_{M \in G} \|[I] - [M] \cdot [Z_n]\|_F^2 = \sum_{i=1}^{N} \min_{m_i \in G_i} \|e_i - m_i \cdot [Z_n]\|_2^2 \tag{7}$$

where G denotes the sparsity pattern constraint, which in some cases is chosen to be the same as that of the original near-field matrix [41], e_i stands for the i-th row of the identity matrix, and m_i is the i-th row of the preconditioning matrix $[M]$. This expression allows good parallelization properties of the SAI preconditioners, since given a number of computing nodes the parallelization process will consist on assigning small and independent LLS problems to each node and gather the results to assemble the preconditioning matrix $[M]$. The ILU preconditioners are typically more difficult to parallelize due to the more sequential nature of the algorithm involved, although parallel implementation details can also be found in the literature [37]. For a given amount of memory (determined by the sparsity pattern) the ILU-based preconditioning approaches typically present faster convergence [40].

4. PARALLELIZATION STRATEGIES

Modern computing hardware architectures are based on multi-node systems that require the parallel programming of EM simulation techniques in order to take full advantage of the computational resources. Parallelization is, thus, a factor that needs to be weighted in when considering the adoption of a numerical technique. Fast algorithms may be discarded and replaced by slower ones that render themselves more scalable.

Aside from the analysis of the scalability of the numerical techniques, the election of the parallelization paradigm is a very important task. The most common models nowadays are the Message Passing Interface (MPI) for distributed memory systems [31], Open Multi-Processing (OpenMP) for shared memory systems [42], and Compute Unified Device Architecture (CUDA) or Open Computing Language (OpenCL) for the parallel application using Graphical Processing Units (GPU) [43]. It is also common to see combinations of these approaches in order to improve the overall performance [44].

Much attention has been paid to the parallelization of the MLFMA approach, especially to simulate very large problems [44, 45]. The load balancing strategies try to distribute the workload equally among all the processing nodes and minimize the communication between them. As a first approach, it is possible to distribute the MLFMA partition groups among the processing nodes. This is only a good solution for the lower levels since these include many groups that can be easily distributed, while at higher levels the number of groups is small, which makes very difficult to find a balanced distribution and some processing nodes may stay idle for extended periods of time. At high levels the number of groups decreases, but, in turn, the size of the groups is larger and so is the number of angular samples required to store and handle the information. To bypass this difficulty the distribution can be a hybridization using the groups at lower levels and the MLFMA angular samples at the higher levels. The level at which the type of distribution switches is called the *translation level*, and it should meet the condition that both the number of blocks per node and the number of samples per node are balanced. At higher levels, a set of adjacent angular samples is assigned to each node to facilitate interpolations using the minimum number of messages between processors, obtaining a load distribution as a set of angular cuts. When, performing the interpolation of an angular value that is close to the border between two processors, the node needs adjacent samples, a message is sent to the corresponding node in order to gather the required data.

While the procedure presented above offers a good balance for an arbitrary number of levels and groups, this partitioning strategy could present some drawbacks when applying the SAI preconditioner using the MPI parallelization. The reason of this burden is based on the distribution of the coefficients of the near-field impedance matrix $[Z_n]$ among the computing nodes. As indicated in a previous section, the SAI preconditioner is calculated from the solution of as many LLS problems as the number of unknowns. Given a subdomain s, its corresponding LLS matrix is built by obtaining the group of subdomains located in the near-field region of s (let G denote this group) and retrieving from $[Z_n]$ all the non-zero reaction terms with any of the subdomains contained in G. This submatrix is usually small and the LLS problems can be calculated very fast, but in a general approach some of the required coefficients may be contained in a different processing node, since $[Z_n]$ is a distributed matrix. In that case it is possible to modify the sparsity pattern of the LLS matrix to ignore those terms and only work with those stored by the parent node, which may result in a poorer performance of the preconditioner. Other alternative consists of the communication of those reaction terms among processors, resulting in a slower computation of the preconditioner but better convergence performance of the system solution. Finally, if a shared parallel strategy is chosen using OpenMP instead of MPI, no time or accuracy penalty will be required, since all the nodes will have full access to any part of $[Z_n]$.

Regarding the scalability of the numerical techniques reviewed in this document, we found that for larger problems the OpenMP implementations of the MoM-MLFMA or MBF approaches are more scalable that the MPI implementations of the same methods. The reason can be the increasing number and size of the messages that need to be exchanged between different nodes in the latter. Using MPI we generally find no improvement in the CPU times when using more than 32 cores, while the efficiency of OpenMP does not seem to degrade even using 114 cores.

5. NUMERICAL EXAMPLES

This section shows test cases simulated using some of the techniques previously mentioned in this document. All the results have been obtained using an HP Z820 Workstation with 16 Intel Xeon E5-2660 processing cores (2.20 GHz) and 128 GBytes of RAM. Unless otherwise indicated, all the examples have been run using 0.25λ as the size of the first level MLFMA regions, an iterative solver (BiCGStab(l) or GMRES(k), indicated in each example) with an error threshold of 10^{-2}, the MPI parallelization paradigm and a sampling rate of 7 divisions per wavelength using basis functions defined over pairs of curved quadrangles that are fully conformed to the surface. A sampling rate of 10 divisions per wavelength would be required to obtain the same accuracy using basis functions defined over pairs of flat triangles. That means that a mesh based on triangles would need about four times more elements than a mesh of quadrangles for the same accuracy. Regarding the number of unknowns a mesh based on flat triangles would require three times more unknowns than a mesh based on curved conformed quadrangles.

For the first test case, the geometry model of a commercial Boeing 757 airplane is shown in Figure 1. The bistatic RCS has been computed at a frequency of 2 GHz using a full-wave CFIE formulation with the Method of Moments combined with the MLFMA. The total number of unknowns of this problem is 5,055,929 (equivalent to about 15 million unknowns using subdomains defined over pairs of flat triangles). The total CPU time spent in the simulation has been 19,395 seconds using the BICGStab
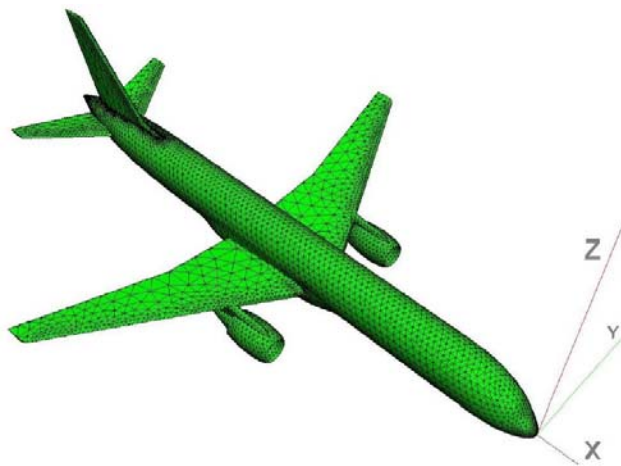
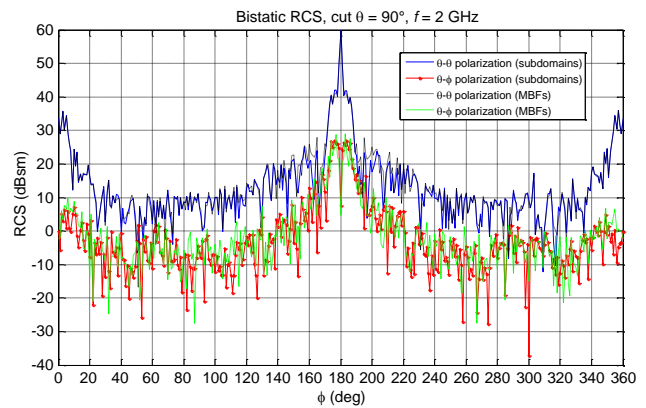**Figure 1.** Model of a Boeing 757 airplane.

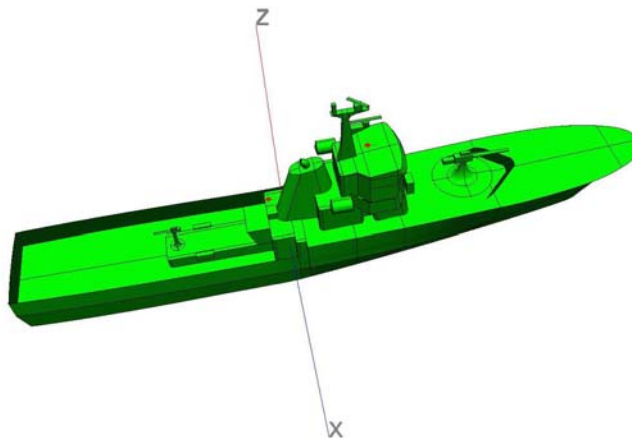**Figure 2.** Bistatic RCS results, $\theta = 90°$ cut.

Figure 3. Geometric model of a patrol boat.

iterative solver without any preconditioner. Convergence has been achieved after 22 iterations. The results are shown in Figure 2 for the $\theta = 90°$ angular cut, and compared with those obtained by the application of the MBF approach. Very good agreement can be noticed between the results obtained from both approaches. This agreement could even improve by considering a higher number of MBFs, as well as by setting a lower error for the iterative solution process. The presented results can be considered a good compromise between the CPU time required for the simulation and the accuracy in the results. The quality of the geometrical model, as well as the mesh generated for the scenario under analysis can also have some impact on the simulation accuracy.

The second example considered in this section involves the patrol boat shown in Figure 3, where two vertical electric dipoles have been placed over the marked spots. A full wave analysis has been performed using the CFIE formulation, resulting 6,522,701 unknowns (equivalent to about 20 million unknowns using subdomains defined over pairs of flat triangles). Figures 4 and 5 show the radiation pattern for the $\phi = 0°$ and $\phi = 90°$ angular cuts. The total CPU time of the simulation for this case has been 58,394 seconds using the BiCGStab solver and no preconditioner. The solver required 72 iterations in this case.

The next example illustrates the benefit obtained by using the MBF approach for the analysis of monostatic RCS scenarios. An almond-shaped geometry, shown in Figure 6, has been analyzed at a frequency of 10 GHz. The total number of basis functions in this case is 321,434 and after the MBF preprocessing 125,282 MBFs have been retained using a block size of one wavelength. A full wave
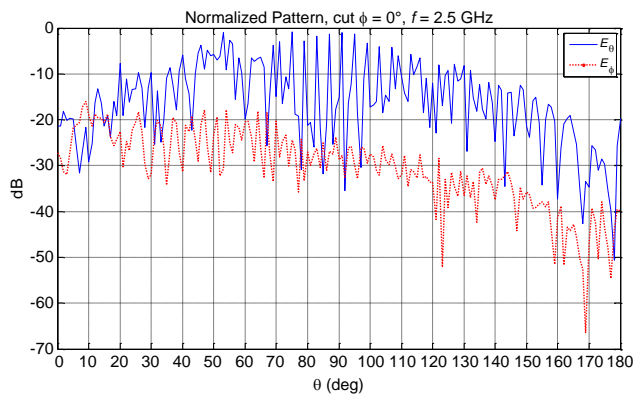

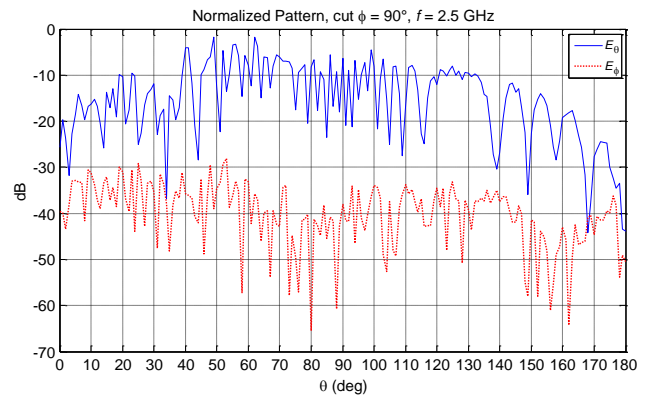**Figure 4.** Radiation pattern results for the $\phi = 0°$ angular cut.

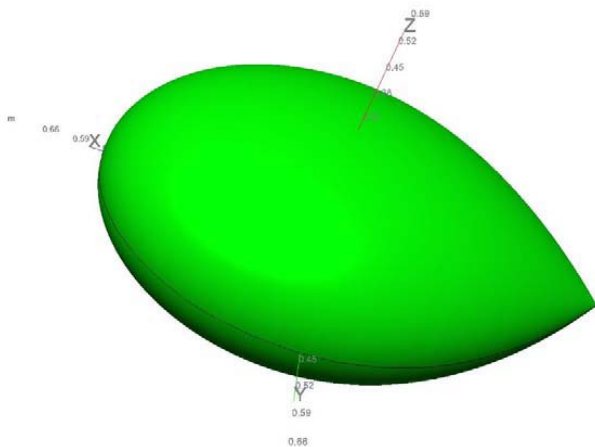**Figure 5.** Radiation pattern results for the $\phi = 90°$ angular cut.

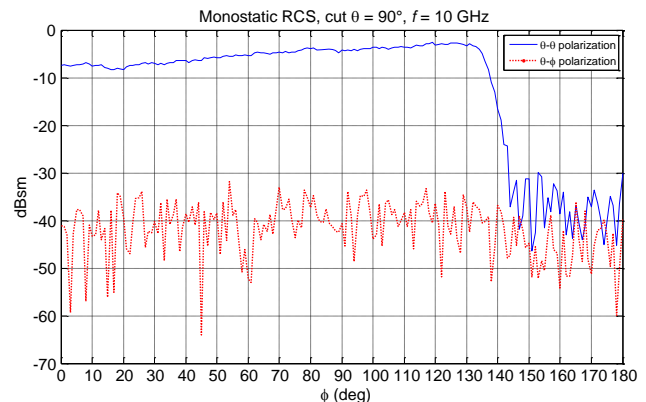**Figure 6.** Almond geometry.

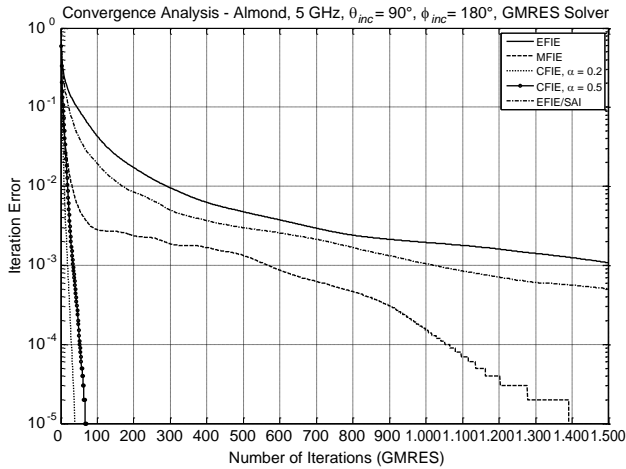**Figure 7.** Monostatic RCS for the $\theta = 90°$ angular cut.

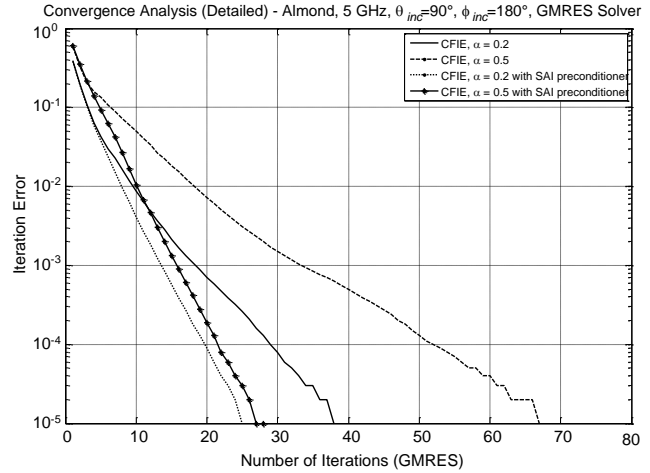**Figure 8.** Convergence analysis for the Almond (5 GHz).

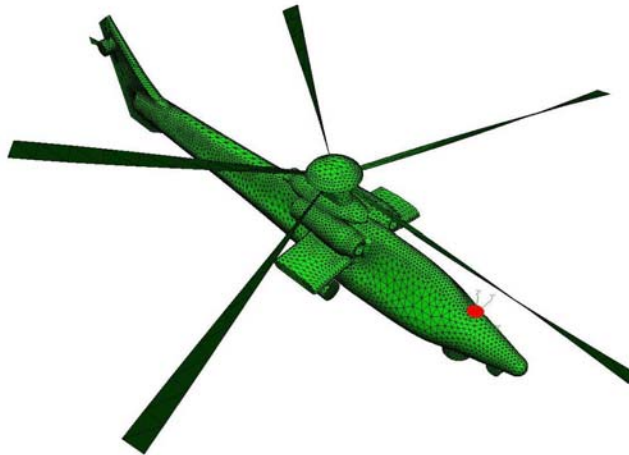**Figure 9.** Detail of the CFIE convergence analysis.

Figure 10. Geometrical model of a helicopter.

analysis has been performed using the CFIE formulation with no preconditioner in order to obtain the monostatic RCS for the $\theta = 90°$ angular cut, with ϕ between $0°$ and $180°$ and θ polarized incident field. The total CPU time has been 6,175 s. An average of 4 iterations has been required by the solver to obtain the results for each incident wave. The computed RCS is shown in Figure 7 for the θ-θ and θ-ϕ polarizations.

A convergence analysis has been performed using this almond-shaped geometry with an incident plane wave propagating along $-\hat{x}$ (towards the tip of the almond) at a frequency of 5 GHz, resulting 81565 unknowns using subdomain basis functions. Figure 8 shows the evolution of the iteration error with the number of iterations for the EFIE, MFIE and CFIE formulations (including $\alpha = 0.2$ and $\alpha = 0.5$), as well as the EFIE with the SAI preconditioner using a sparsity distance of 0.25λ. A much faster convergence is achieved with CFIE, which is further detailed in Figure 9, including the use of the SAI preconditioner as well, that contributes to a faster convergence and allows an iteration error below 10^{-5} in less than 30 iterations.

Figure 10 shows the model of a helicopter where a vertical electric dipole has been placed near the nose. This case has been simulated at 1.5 GHz in order to obtain the radiation pattern of the on-board antenna. The total size of the problem is 400,488 unknowns, and the simulation requires 4,123 seconds using the EFIE formulation, since the geometry contains open surfaces. The SAI preconditioner and the

GMRES(300) solver have been applied in this case. Figures 11 and 12 show the results for the $\theta = 90°$ and then $\phi = 0°$ angular sweeps. Convergence has been achieved after 422 inner iterations, including the restart after 300 iterations.

For the next test case, the scenario depicted in Figure 13 has been considered. It includes the helicopter shown in Figure 10 with the patrol boat. The excitation is the dipole on board of the helicopter, considering no other sources on the surface of the boat. The simulation of this scenario has been performed at a frequency of 1.5 GHz using the EFIE formulation, resulting 2,725,776 unknowns from the discretization process. The full-wave analysis of this problem requires 30509 seconds using the GMRES(300) solver and the SAI preconditioner after 705 iterations and the results, computed for the $\theta = 90°$ angular cut, have been compared with those obtained by using an alternative approach, consisting on the simulation of the helicopter isolated and the substitution of the helicopter in the scene by its multipole expansion as a complex set of sources. This new approach can be seen in Figure 14. In this representation of the source the side length of the cubes used for the multipole model is 4λ. While the simulation of the full physical scenario is preferable when a strong interaction between the source surface and the rest of the geometry is expected, the use of a complex source is more accurate than a single source when there are other structures in its vicinity which are not strongly coupled to the source surface, and this approach can greatly speed up the simulation. Figures 15 and 16 show the excellent agreement of the results of the full-wave simulation and the approach based on the substitution of the
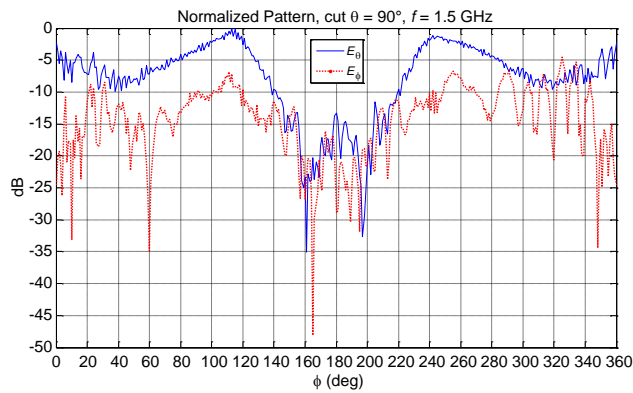

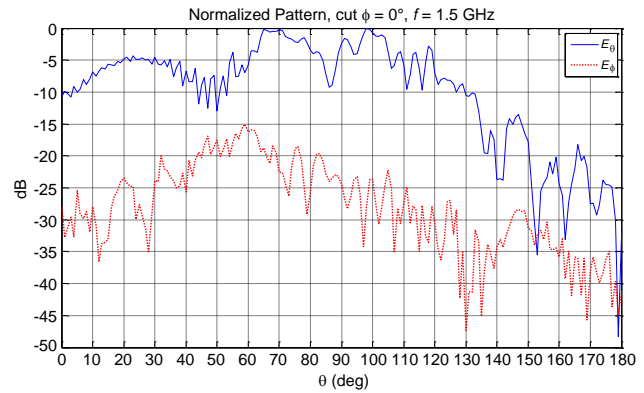**Figure 11.** Radiation pattern for the $\theta = 90°$ angular cut.

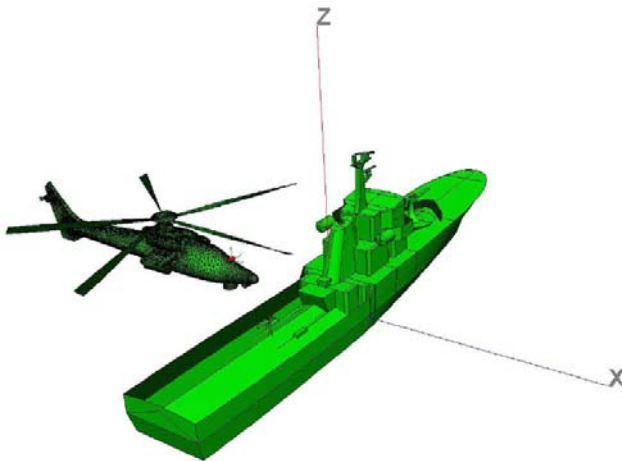**Figure 12.** Radiation pattern for the $\phi = 0°$ angular cut.

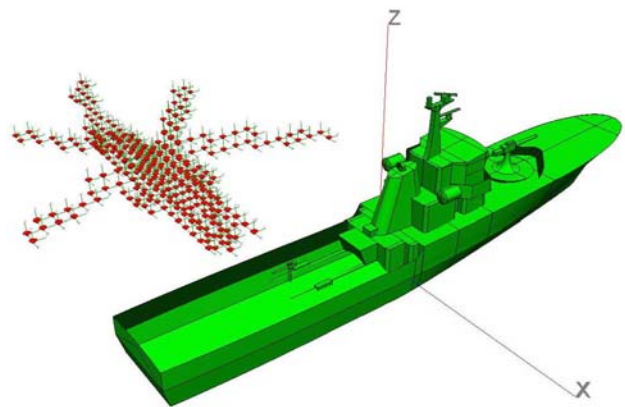**Figure 13.** Geometrical model of a helicopter close to a patrol boat.

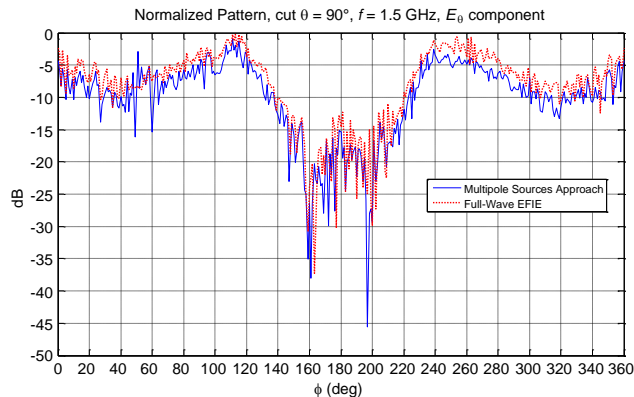**Figure 14.** The helicopter has been replaced by a multipole expansion.

Figure 15. Radiation pattern for the $\theta = 90°$ angular cut, E_θ component.
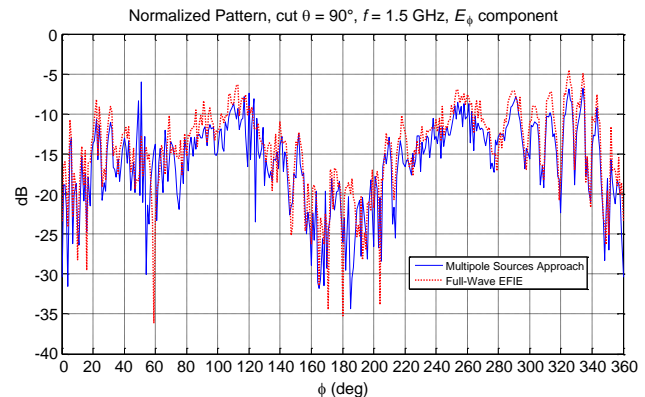
Figure 16. Radiation pattern for the $\theta = 90°$ angular cut, E_ϕ component.

helicopter by its multipole expansion. The CPU time of this approach is 16871 seconds, and including the time spent in the simulation of the helicopter isolated the total time is 20904 seconds, noticeably smaller than the time required for the computation of the full scenario. As with the full scenario, the SAI preconditioner and the GMRES(300) solver have been used in this case, requiring 251 iterations.

6. CONCLUDING REMARKS

Some of the modern techniques used in the computation of electromagnetic problems have been presented in the present document. The goal of most of the modern approaches is the reduction of the computational requirements while maintaining a high degree of accuracy. For this purpose this techniques avoid the storage of the far-field interactions between basis functions, perform fast matrix-vector multiplications in the solution process and/or reduce the number of unknowns by introducing specific macro-basis functions tailored to individual blocks. These numerical approaches, together with the use of preconditioners and efficient parallelization strategies, allow the solution of realistic problems with limited resources. A number of test cases have been chosen to demonstrate the capabilities of these methods to address different types of problems. It seems natural to estimate that in future years the tendency will continue to favor full-wave analysis of larger problems using more powerful hardware where the scalability of the numerical techniques will play a critical role due to the high number of processing cores involved. It can be remarked, however, that at the core of each one of these MoM-based methods it is always possible to find the direct application of Maxwell's equations.

ACKNOWLEDGMENT

REFERENCES

1. Maxwell, J. C., "A dynamical theory of the electromagnetic field," *Philosophical Transactions of the Royal Society of London*, Vol. 155, 459–512, 1865.

2. Kouyoumjian, R. G., "Asymptotic high-frequency methods," *Proceedings of the IEEE*, Vol. 53, No. 8, 864–876, Aug. 1965.

3. Knott, E. F., "A progression of high-frequency RCS prediction techniques," *Proceedings of the IEEE*, Vol. 73, No. 2, 252–264, Feb. 1985.

4. Harrington, R. F., *Field Computation by Moment Methods,* McMillan, New York, 1968.

5. Chew, W. C., J.-M. Jin, C.-C. Lu, E. Michielssen, and J. Song, *Fast and Efficient Algorithms in Computational Electromagnetics*, Artech House, 2001.

6. Rao, S. M., D. R. Wilton, and A. W. Glisson, "Electromagnetic scattering by surfaces of arbitrary shape," *IEEE Trans. Antennas Propagat.*, Vol. 30, No. 3, 409–412, May 1982.

7. Glisson, A. W. and D. R. Wilton, "Simple and efficient numerical methods for problems of electromagnetic radiation and scattering from surfaces," *IEEE Trans. Antennas Propagat.*, Vol. 28, No. 5, 593–603, Sep. 1980.

8. Engheta, N., W. D. Murphy, V. Rokhlin, and M. S. Vassiliou, "The fast multipole method (FMM) for electromagnetic scattering problems," *IEEE Trans. Antennas Propagat.*, Vol. 40, No. 6, 634–641, Jun. 1992.

9. Coifman, R., V. Rokhlin, and S. Wandzura, "The fast multipole method for the wave equation: A pedestrian prescription," *IEEE Antennas and Propagation Magazine*, Vol. 35, No. 3, 7–12, Jun. 1993.

10. Chew, W. C., J.-M. Jin, C.-C. Lu, E. Michielssen, and J. Song, "Fast solution methods in electromagnetics," *IEEE Trans. Antennas Propagat.*, Vol. 45, No. 3, 533–543, 1997.

11. Burkholder, R. and J. F. Lee, "Fast dual MGS block-factorization algorithm for dense MoM matrices," *IEEE Trans. Antennas Propagat.*, Vol. 52, No. 7, 1693–1699, 2004.

12. Ozdemir, N. A. and J. F. Lee, "A low rank IE-QR algorithm for matrix compression in volume integral equations," *IEEE Trans. Magn.*, Vol. 40, No. 2, 1017–1020, 2004.

13. Zhao, K., M. N. Vouvakis, and J.-F. Lee, "The adaptive cross approximation algorithm for accelerated method of moments computations of EMC problems," *IEEE Trans. Electromag. Compat.*, Vol. 47, No. 4, 763–773, 2005.

14. Laviada, J., R. Mittra, M. R. Pino, and F. Las-Heras, "On the convergence of the ACA," *Microwave Opt. Technol. Lett.*, Vol. 51, No. 10, 2458–2460, 2009

15. Heldring, A., E. Ubeda, and J. M. Rius, "On the convergence of the ACA algorithm for radiation and scattering problems," *IEEE Trans. Antennas Propag.*, Vol. 62, No. 7, 3806–3809, 2014.

16. Tamayo, J., A. Heldring, and J. Rius, "Multilevel adaptive cross approximation (MLACA)," *IEEE Trans. Antennas Propagat.*, Vol. 59, No. 12, 4600–4608, 2011.

17. Schroder, A., H.-D. Bruns, and C. Schuster, "Fast evaluation of electromagnetic fields using a parallelized adaptive cross approximation," *IEEE Trans. Antennas Propagat.*, Vol. 62, No. 5, 2818–2822, 2014.

18. Schroder, A., H.-D. Bruns, and C. Schuster, "A hybrid approach for rapid computation of two-dimensional monostatic radar cross section problems with the multilevel fast multipole algorithm," *IEEE Trans. Antennas Propagat.*, Vol. 60, No. 12, 6058–6061, 2012.

19. Maaskant, R., R. Mittra, and A. Tijhuis, "Fast analysis of large antenna arrays using the characteristic basis function method and the adaptive cross approximation algorithm," *IEEE Trans. Antennas Propagat.*, Vol. 56, No. 11, 3440–3451, 2008.

20. Boag, A. and R. Mittra, "Complex multipole beam approach to electromagnetic scattering problems," *IEEE Trans. Antennas Propagat.*, Vol. 42, No. 3, 366–372, 1994.

21. Tap, K., P. H. Pathak, and R. J. Burkholder, "Complex source beam-moment method procedure for accelerating numerical integral equation solutions of radiation and scattering problems," *IEEE Trans. Antennas Propagat.*, Vol. 62, No. 4, 2052–2062, 2014.

22. Canning, F. X., "The impedance matrix localization (IML) method for method of moment calculations," *IEEE Antennas and Propagation Magazine*, Vol. 32, 18–30, 1990.

23. Bleszynski, E., M. Bleszynski, and T. Jaroszewcz, "AIM: Adaptive integral method compression algorithm for solving large scale electromagnetic scattering and radiation problems," *Radio Sci.*, Vol. 31, 1225–1251, 1996.

24. Michelsen, E. and A. Boag, "A multilevel matrix decomposition algorithm for analyzing scattering from large structures," *IEEE Trans. Antennas Propagat.*, Vol. 44, No. 8, 1086–1093, Aug. 1996.

25. Prakash, V. V. S. and R. Mittra, "Characteristic basis function method: A new technique for efficient solution of method of moments matrix equation," *Microwave Opt. Technol. Lett.*, Vol. 36,

No. 2, 95–100, Jan. 2003.

26. Delgado, C., F. Cátedra, and R. Mittra, "Application of the characteristic basis function method utilizing a class of basis and testing functions defined on NURBS patches," *IEEE Trans. Antennas Propagat.*, Vol. 56, No. 3, 784–791, Mar. 2008.

27. Matekovits, L., V. A. Laza, and G. Vecchi, "Analysis of large complex structures with the synthetic-functions approach," *IEEE Trans. Antennas Propagat.*, Vol. 55, No. 9, 2509–2521, Sep. 2007.

28. Delgado, C., R. Mittra, and F. Cátedra, "Accurate representation of the edge behavior of current when using PO-derived characteristic basis functions," *IEEE Antennas and Wireless Propagation Letters*, Vol. 7, 43–45, Mar. 2008.

29. García, E., C. Delgado, I. González, and F. Cátedra, "An iterative solution for electrically large problems combining the characteristic basis function method and the multilevel fast multipole algorithm," *IEEE Trans. Antennas Propagat.*, Vol. 56, No. 8, 2363–2371, 2008.

30. Blackford, L. S., J. Choi, A. Cleary, E. D'Azevedo, J. Demmel, I. Dhillon, J. Dongarra, S. Hammarling, G. Henry, A. Petitet, K. Stanley, D. Walker, and R. C. Whaley, *ScaLAPACK Users' Guide*, SIAM, 1997.

31. Traff, J. L., W. D. Gropp, and R. Thakur, "Self-consistent MPI performance guidelines," *IEEE Trans. Parallel and Distributed Systems*, Vol. 21, No. 5, 698–709, May 2010.

32. Saad, Y., *Iterative Methods for Sparse Linear Systems,* 2nd Edition, SIAM, Philadelphia, 2003.

33. Van der Vorst, H. A., "Bi-CGSTAB: A fast and smoothly converging variant of Bi-CG for the solution of nonsymmetric linear systems," *SIAM J. Sci. and Stat. Comput.*, Vol. 13, No. 2, 631–644, 1992.

34. Saad, Y. and M. H. Schultz, "GMRES: A generalized minimal residual algorithm for solving nonsymmetric linear systems," *SIAM J. Sci. and Stat. Comput.*, Vol. 7, 856–869, 1986.

35. Kharchenko, S. A. and A. Yu. Yeremin, "New GMRES(k)-type algorithms with explicit restarts and the analysis of their convergence properties based on matrix relations in QR form," *Journal of Mathematical Sciences*, Vol. 114, No. 6, 2003.

36. Canning, F. X. and J. F. Scholl, "Diagonal preconditioners for the EFIE using a wavelet basis," *IEEE Trans. Antennas Propagat.*, Vol. 44, No. 9, 1239–1246, 1996.

37. Lee, J., C.-C. Lu, and J. Zhang, "Incomplete LU preconditioning for large scale dense complex linear systems from electromagnetic wave scattering problems," *J. Comp. Phys.*, Vol. 185, 158–175, 2003.

38. Kolotilina, L. Y., "Explicit preconditioning of systems of linear algebraic equations with dense matrices," *Journal of Soviet Mathematics*, Vol. 43, No. 4, 2566–2573, Nov. 1988.

39. Carpentieri, B., I. S. Duff, L. Giraud, and G. Sylvand, "Combining fast multipole techniques and an approximate inverse preconditioner for large electromagnetism calculations," *SIAM J. Sci. and Stat. Comput.*, Vol. 27, No. 3, 774–792, 2006.

40. Benzi, M. and M. Tuma, "A comparative study of sparse approximate inverse preconditioners," *Applied Numerical Mathematics: Transactions of IMACS*, Vol. 30, Nos. 2–3, 305–340, 1999.

41. Lee, J., C.-C. Lu, and J. Zhang, "Sparse inverse preconditioning of multilevel fast multipole algorithm for hybrid integral equations in electromagnetics," *IEEE Trans. Antennas Propagat.*, Vol. 52, No. 9, 2277–2287, 2004.

42. Chapman, B., G. Jost, and R. van der Pas, *Using OpenMP: Portable Shared Memory Parallel Programming,* MIT Press, Oct. 2007.

43. Lezar, E. and D. B. Davidson, "GPU-accelerated method of moments by example: Monostatic scattering," *IEEE Antennas and Propagation Magazine*, Vol. 52, No. 6, 120–135, 2010.

44. Pan, X. M., W. C. Pi, M. L. Yang, Z. Peng, and X. Q. Sheng, "Solving problems with over one billion unknowns by the MLFMA," *IEEE Trans. Antennas Propagat.*, Vol. 60, No. 5, 2571–2574, 2012.

45. Ergul, O. and L. Gurel, "Accurate solutions of extremely large integralequation problems in computational electromagnetics," *Proceedings of the IEEE*, Vol. 101, No. 2, 342–349, 2013.